AN ABSTRACT OF THE THESIS OF

Richard James Baumann for the degree of Master of Science

in the School of Oceanography presented on July 17, 1978

Title: An Analysis of One Year of Surface Layer Meteorological Data from the Arctic Pack Ice

Abstract approved: Redacted for Privacy

Clayton A. Paulson

The thesis describes the properties of surface wind and air temperature time series recorded at three locations on the pack ice of the Beaufort Sea. Time series consisting of sequential one-half hourly means were constructed for a period of approximately a year. A diurnal fluctuation in air temperature is found for the late summer, early fall and spring seasons only. Wind speed does not show a significant diurnal fluctuation for any season. There is very little seasonal variability in the wind speed while significant variation is present in the air temperature. The integrated wind speed spectrum (i.e. variance) is 80% less than the integrated sum of the wind component spectra indicating that for periods longer than a day, directional fluctuations contribute much more to the variance of the wind record than do speed fluctuations. Although the measurements only approach the microscale region, there seems to be no consistent indication of a microscale peak in the variance preserving representation of the

wind speed spectrum. Time series of daily mean horizontal divergence and vertical component of vorticity for both the wind field and ice motion are examined. For a period of 355 days there is significant negative correlation (-0.65) between the wind divergence and wind vorticity series and significant positive correlation (0.65) between the wind vorticity and ice vorticity series.

An Analysis of One Year of Surface Layer Meteorological Data from the Arctic Pack Ice

by

Richard James Baumann

A THESIS

submitted to

Oregon State University

in partial fulfillment of
the requirements for the
degree of

Master of Science

Completed July 17, 1978

Commencement June 1979

APPROVED:

Redacted for Privacy

Associate Professor of Oceanography
in charge of major

Redacted for Privacy

Acting Dean of School of Oceánography

Redacted for Privacy

Dean of Graduate School

Date thesis is presented July 17, 1978

Typed by Margi Wolski for Richard James Baumann

TABLE OF CONTENTS

LIST OF FIGURES

List of Figures, continued.

LIST OF TABLES

AN ANALYSIS OF ONE YEAR OF SURFACE LAYER METEOROLOGICAL DATA FROM THE ARCTIC PACK ICE

1. INTRODUCTION

1.1 Preview

Wind and air temperature time series recorded over land have been analyzed by numerous investigators (e.g. Hwang, 1970; Lyons, 1975; Oort and Taylor, 1969; Van der Hoven, 1957; and Panofsky, 1969) to determine synoptic and mesoscale (as defined in Table I) characteristics. However, over topographically flat surfaces such as the open ocean or sea ice the number of observations of these variables and the resulting analyses is significantly smaller (e.g. Dorman, 1974; Millard, 1971; and Burt et al., 1974).

One goal of the Arctic Ice Dynamics Joint Experiment (AIDJEX) was to gain a better understanding of the wind and air temperature fields over the pack ice in the Beaufort Sea (Maykut et al., 1972). In this work advantage is taken of the unique opportunity to analyze the time series of these variables that were recorded at three different manned camps during the year-long AIDJEX main experiment. The time series are discussed and related to the general climatology of the Arctic basin. The power spectra of the wind and air temperature fields are presented and compared to the results of other investigators. The 24-hour mean horizontal divergence and vertical component of

TABLE I. Definition of Scales (after Fiedler and Panofsky, 1970).

	Microscale	Mesoscale	Synoptic Scale
Period	< 1 hr	1 hr - 48 hr	> 48 hr
Wavelength	< 20 km	20 km - 500 km	>500 km

vorticity for both the ice motion and the wind field are discussed and related to each other.

1.2 The Polar Ocean and Its Climate

One can view the global atmospheric circulation system as being the result of the latitudinal variation of the solar heating of the surface of a rotating earth. The atmosphere and the world oceans transport the excess heat gained in the low latitudes to the polar regions where it is lost to space to achieve the heat balance which is nearly steady when averages over periods longer than a year are taken. In the mid-latitudes, synoptic weather systems control the weather and climate through a constantly evolving system of mobile air masses resulting from the latitudinal variation of solar heating and the differential heating and cooling of the land and water surfaces. In the Arctic, however, there is little of the air mass phenomena necessary for cyclonic development and those cyclonic patterns that do evolve or migrate in from outside the region generally have little influence on the climate, other than controlling the turbulence in the inversion layer.

The lower troposphere in the Arctic is usually characterized by a temperature inversion (no month of the year shows inversions present less than 59% of the time while in winter this often reaches 100%) which can be divided into three types; relatively shallow, radiation

inversions which are established by the heat loss at the surface; subsidence inversions created by large scale dynamic effects; and advection inversions usually resulting from the advection of warmer air over the underlying colder surface air mass in summer (Vowinckel and Orvig, 1970). In winter a positive vertical temperature gradient between the surface and 850 millibars (1.5 km) as high as 10°C has been found over the Beaufort Sea, while in summer only a slight positive gradient is found (Vowinckel and Orvig, 1970). In temperate latitudes warm and cold spells are normally caused by radiation rather than by advection. A break-down of the inversion layer and the resulting downward transport of warmer air is required for milder surface temperatures.

Depending on the season, 85% to 99% of the Polar Ocean is covered with a layer of sea ice ranging in thickness from a few millimeters to six or seven meters. The average thickness has been estimated to be between two and three meters (Vowinckel and Orvig, 1970). The ice cover in winter serves to insulate the relatively warm ocean water (-1.6°C) from the colder atmosphere (-20°C to -40°C) which has been established by the radiation balance. In summer the melting ice surface keeps the surface temperature from rising above 0°C.

1.3 Data Collection

The AIDJEX main experiment took place on the pack ice of the Beaufort Sea from April, 1975 to April, 1976. Initially an array was established (Figure 1) in the form of an approximate equilateral triangle with a manned camp at each vertex and one in the center (which had to be abandoned halfway through the experiment). The data reported here are from the three camps (Caribou, Bluefox, and Snowbird) that existed for the entire experiment. At the time it was established, the length of the sides of the array varied from 125 to 175 kilometers, but by the end of the experiment the original equilateral form had been distorted until the length of the sides varied from 90 to 300 kilometers. During the year, movement of the pack ice carried the entire array approximately 400 kilometers to the south/southeast.

At each camp there was a ten-meter tower from which air temperature at the heights of two and nine meters and instantaneous and time-averaged (60 second time constant) wind speed and direction at ten meters height were measured. The signals were digitally sampled once every 30 seconds for the entire year except for periods ranging from several minutes to eight days when data were not collected at one or another of the camps. The handling of these gaps in the record is discussed in the next section. The temperature

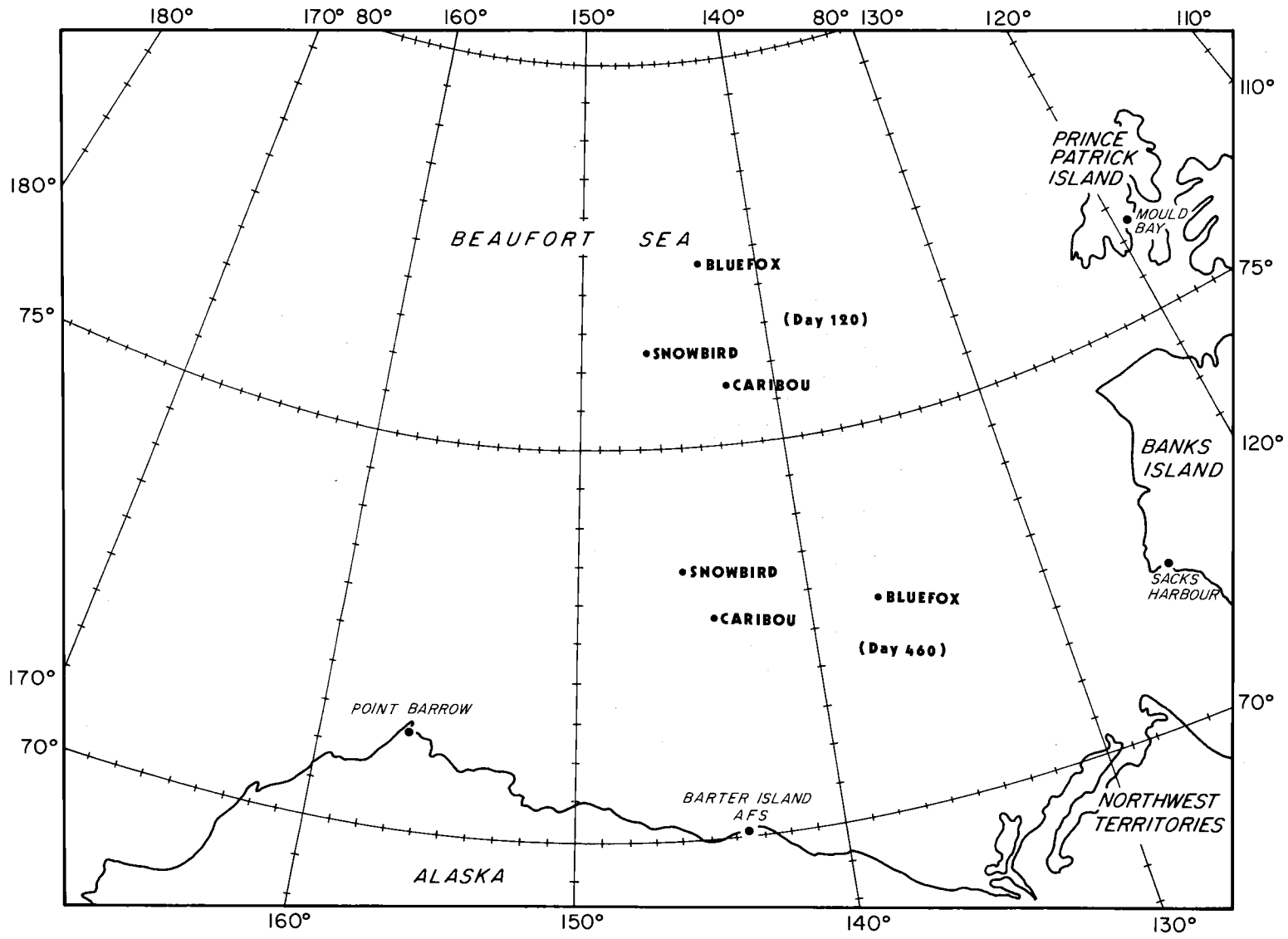

Figure 1. Location of the AIDJEX manned camp array at the beginning and end of the year-long AIDJEX main experiment.

sensors were platinum resistance elements inside aspirated radiation shields. The wind sensors were three cup anemometers and vanes. Pertinent information regarding the sensors is summarized in Table II.

The output of the sensors was converted to a voltage between zero and five volts by a Climet model 060-10A translator. The data were recorded in digital form on magnetic tape by a Nova 2 minicomputer through a ten bit analog-to-digital converter. This provided for a resolution of five millivolts or $\pm$ 0.08°C in temperature, $\pm$ 0.02 m s^{-1} in wind speed and $\pm$ 0.35 degrees in wind direction. Each channel of information was also recorded once every 20 minutes as a voltage printed on paper tape. The temperature signals and the time averaged wind speed and direction were also recorded continuously on strip chart recorders. More detailed information concerning the description of the data collection system and its performance can be found in Paulson and Bell (1975) and Clarke et al. (1977).

1.4 Data Preparation

One-half hour means of air temperature at two and nine meters, wind speed from both the instantaneous and time averaged signals, and u and v wind components were constructed from the raw data which was sampled every 30 seconds. The instantaneous wind speed and direction were used to calculate u and v wind components which were

TABLE II. Sensor Specifications (All sensors manufactored by Climet).

Variable	Sensor	Range	Instrument accuracy
Temperature 2 m and 9 m	Shield - model 016-1 Sensor - model 014-74	-60 to 20° C	$\pm$ 0.05° C
Wind Speed	Model 011-1	0.25 to 22.4 m s^{-1}	the greater of $\pm$ 1% or 0.07 m s^{-1}
Wind Direction	Model 012-30	0 to 360°	$\pm$ 2°

then averaged to form the one-half hour means. Since the camps were on ice floes that rotated, a time varing correction had to be applied to the local wind vectors to correctly decompose then into a North-South coordinate system. Time averaged wind direction was not used in the analysis because it was often contaminated by the wind vane signal changing from zero to five volts as the direction varied around the local 0 and 360°.

For periods of six hours and less where data were missing from the tapes recorded in the field, a linear interpolation was employed to generate the needed one-half hour means. Periods of missing data longer than six hours were filled using the values recorded on paper tape. For longer periods during which data were not recorded either on magnetic or paper tape (as happened at Snowbird where there are five periods ranging in length from one to eight days where there were not data), means from one of the other camps were used to fill the gaps. Corrections were made for bad data points resulting from radio and aircraft beacon interference and other obvious noise. A comprehensive discussion of the editing that went into the one-half hour means and a complete listing of those means that were corrected can be found in Baumann (1978).

From the one-half hour means, 3, 6, 12, and 24-hour means were calculated. The means from the three camps are synchronous in time. Time series of camp motion, camp position, and wind direction

correction information were obtained from the AIDJEX data bank and have been used in the analysis.

Several factors have been identified as sources of error in the data. Rime ice forming on the sensors was a problem, particularly in the fall. Heavy accumulations were often found on the wind speed and direction sensors which caused systematic errors in the data being recorded. The temperature sensors were occasionally found clogged with hoarfrost which prevented proper aspiration. This allowed radiative heating of the sensor housing and the platinum resistance element itself. Hoarfrost also affected the wind sensors. By searching through the daily meteorological logs, periods where these problems were present were avoided in the analysis of the 30 second per sample data. These problems were not corrected in the process of calculating the one-half hour means. The sensors were cleaned at least twice a day and more often when conditions warranted it. The overall effect of these problems is not large when the year-long series is considered, although for short periods the errors may be considerable.

2. THE TIME SERIES

2.1 Preview

The meteorological time series collected during the AIDJEX main experiment constitute one of the most complete sets of meso-scale wind and air temperature data available for the Arctic. These time series provide the data needed to check the predictions of the model of the Arctic atmospheric boundary layer used to calculate the air stress on the pack ice. Such factors as the effect of atmospheric stability on the angle between the geostrophic wind and the surface wind, the time-scales at which most variance or power is present in the wind field, and the relationship between the horizontal divergence and the vertical component of vorticity of the wind field and the ice motion itself are all important in the modeling of ice motion, the primary objective of the AIDJEX program.

In the following sections the time series are examined as to their variability with the season of the year, their mean statistics, and the differences between the series calculated for each of the three camps. In the following, the caption AIDJEX DAYS refers to the Julian day for 1975 and the Julian day plus 365 for 1976 (i.e., day 120 is 30 April 1975 and day 475 is 19 April 1976; a conversion table is provided in Appendix I).

2.2 Series of 24-Hourly Means

Figure 2 presents a 365 point series of 24-hour mean air temperature at two meters height and wind speed for Snowbird and for the three-camp average. As is readily apparent the yearly signal is dominant in the air temperature record. Also evident on this is the almost constant summer temperature of 0°C resulting from the inability of the surface temperature to rise above the melting point. The wind speed time series show a slight rise in average wind speed during the fall and early winter. An important point to note is that for 24-hour averaging intervals, the records of the three camps are nearly identical in their frequency content and have only minor variations in their levels.

The yearly three-camp averages are wind speed, 4.8 m s^{-1}; air temperature at two meters, -17.9°C, and air temperature at nine meters, -17.7°C.

Wind direction is a difficult variable to display on a synoptic or longer time scale. An attempt to reflect the directional content of the wind record is made in Figure 3. These wind roses were computed from 24-hour mean wind vectors for days 120 to 475. With the exception of south and southeast, the wind directions are fairly evenly distributed over all eight points of the compass. Referring

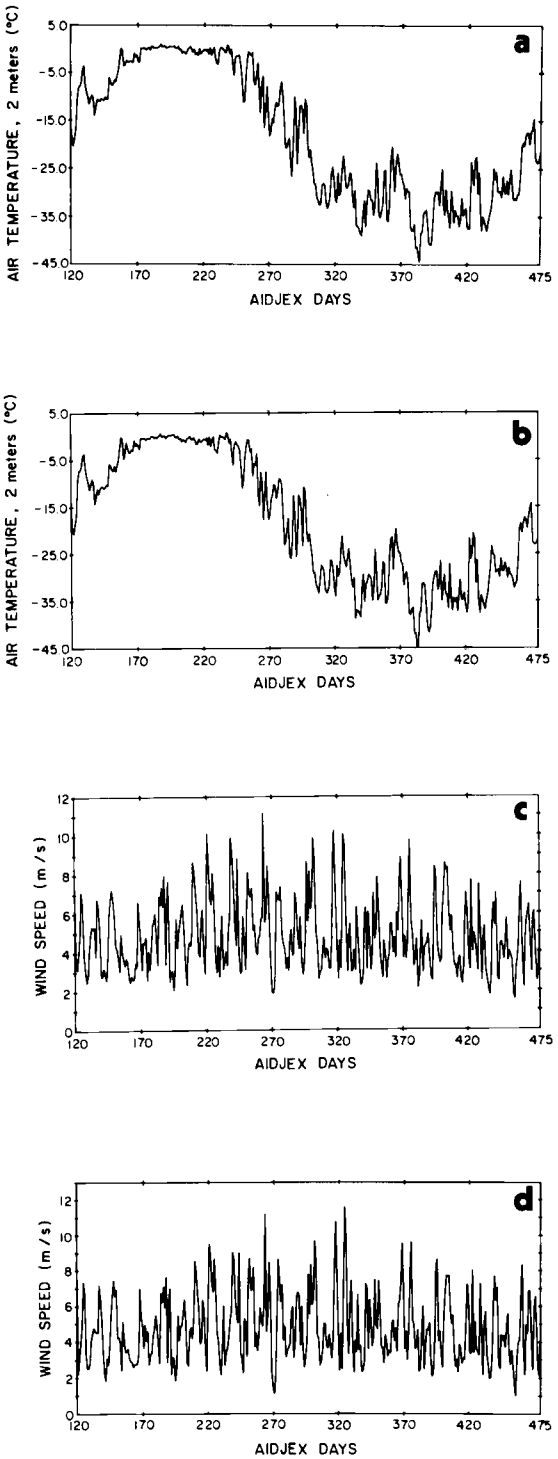

Figure 2. Daily mean values of wind speed and air temperature from Snowbird, (a) and (c), and the average for all three camps, (b) and (d).

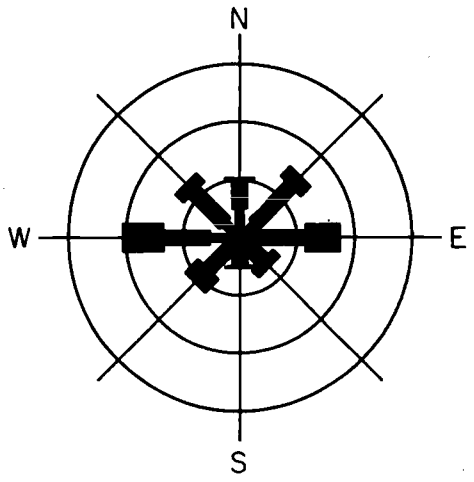

CARIBOU

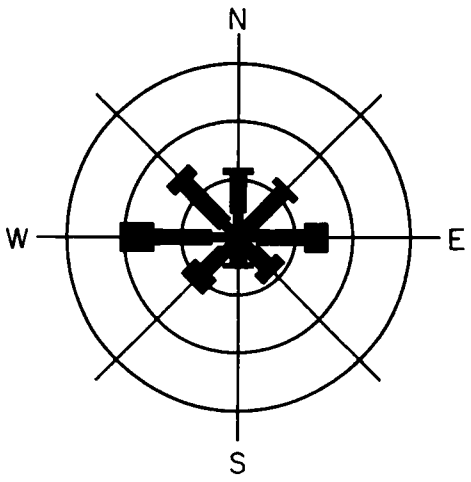

BLUEFOX

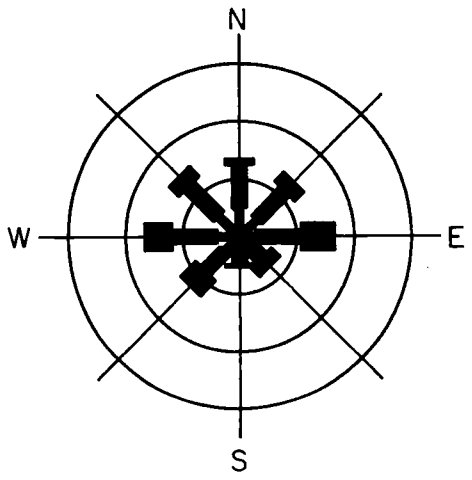

SNOWBIRD

Each ring represents 10% of the total wind record.

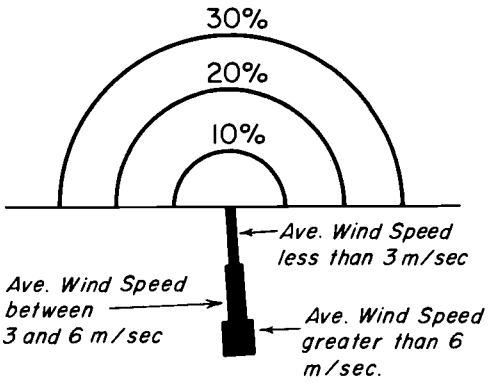

For each direction Wind Speed is sorted into three speed bands; 0-3, 3-6, greater than 6 m/sec.

Figure 3. Yearly wind roses calculated from the daily mean vector wind. Directions is in the meteorological sense (i.e., the direction from which the wind is blowing).

back to Figure 1, this is the direction the camps are seen to move during the year the array was in existence.

2.3 Series of One-half Hourly Means

Much of the analysis contained in this study has been performed using the time series of one-half hourly means. In Figures 4 and 5, the same 10 days of data from Caribou and Bluefox for two different periods of the experiment are presented. Figure 4 is from the summer of 1975 and Figure 5 is from the fall. The wind speed records are very similar for these two different seasons. The temperature records vividly display the contrast between the summer melt period and the colder fall season.

2.4 Series Sampled at 30-Second Intervals

The data were acquired in the field at a sampling rate of two samples per minute. Two 256-minute records of the data from Bluefox are shown in Figure 6. As in the previous examples, the summer temperature is seen to be fairly constant when compared to that from the fall. Both temperature records show the limitation of the $\pm$ 0.08°C resolution of the data acquisition system that precluded a spectral analysis of the 30-second temperature data. The wind speed records do not display any significant differences that can be related

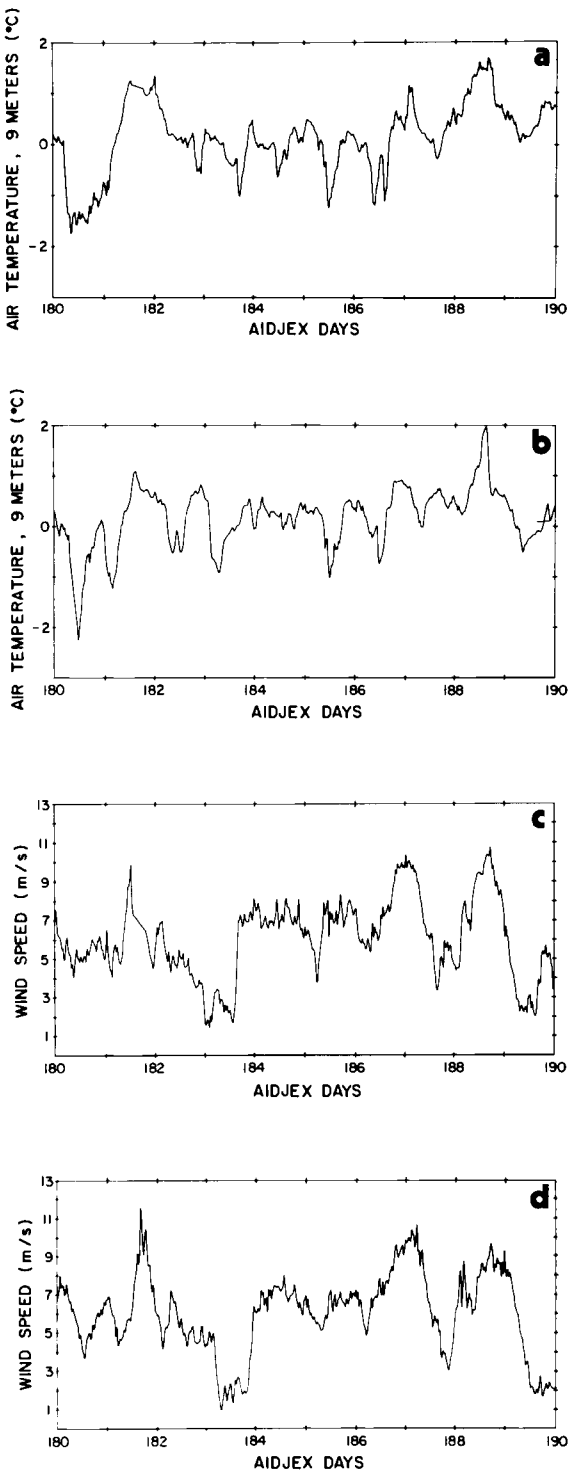

Figure 4. Time series of one-half hourly mean air temperature and wind speed for the period 29 Jun. 75 to 9 Jul. 75 from Caribou, (a) and (c), and Bluefox, (b) and (d).

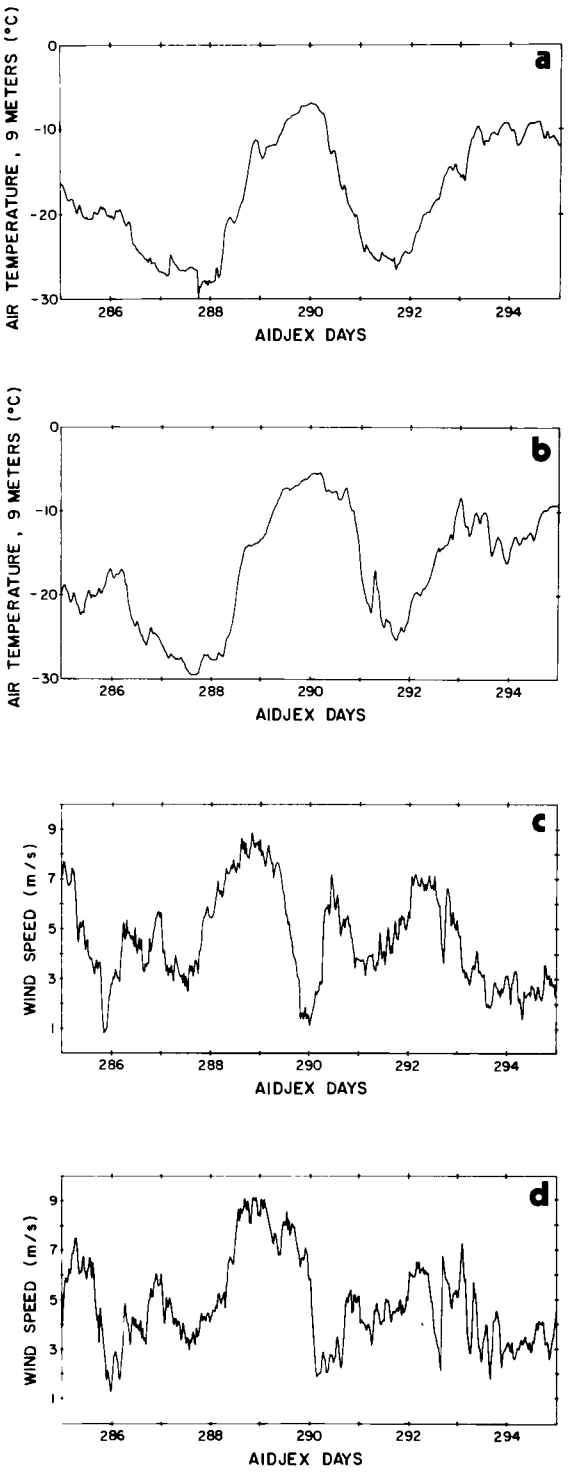

Figure 5. Time series of one-half hourly mean air temperature and wind speed for the period 12 Oct 75 to 22 Oct 75 from Caribou, (a) and (c), and Bluefox, (b) and (d).

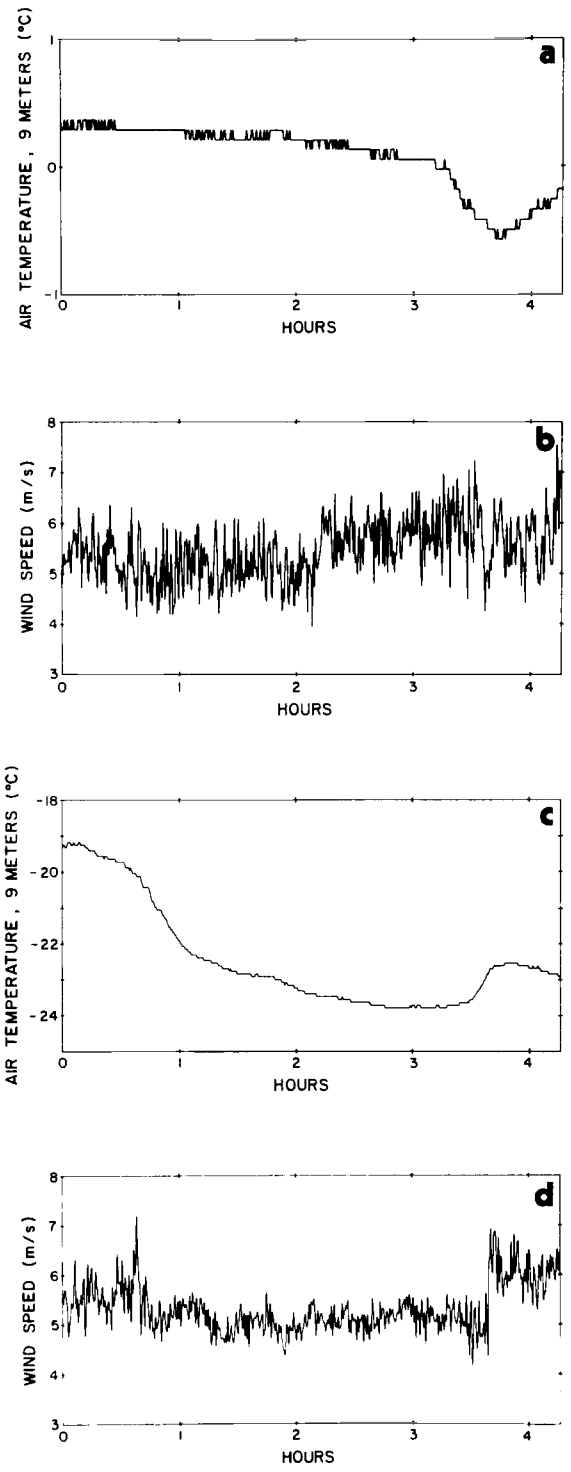

Figure 6. Wind speed and air temperature sampled twice per minute from Bluefox for (a) and (b) 4 Jul 75, (c) and (d) 18 Oct 75.

to the time of year. The jump of about 1.5 m s^{-1} in the wind speed record for 18 October was caused by the cleaning of rime ice off the sensor.

3. SPECTRAL ANALYSIS

3.1 The Theory and Its Application

Spectral analysis is a method by which a time series can be written as the sum of a set of cosine functions of differing frequency and phase. Each cosine function is multiplied by an amplitude factor whose square can be viewed as representing the contribution to the total variance present at a particular frequency. If we have a time series of N points,

$$[X_k], \quad k = 1,2,\ldots,N$$

the Fourier analysis used in spectral computations provide the coefficients a_n and b_n such that

$$X_k = a_0 + \sum_{n=1}^{N/2} C_n \cos\left(\frac{2\pi nk}{N} + \theta_n\right)$$

where

$$a_0 = \frac{1}{N} \sum_{k=1}^{N} X_k$$

$$c_n = (a_n^2 + b_n^2)^{1/2}$$

$$\theta_n = \mathrm{Tan}^{-1}\left(-\frac{b_n}{a_n}\right)$$

$$a_n = \frac{2}{N} \sum_{k=1}^{N} X_k \cos\frac{2\pi nk}{N}$$

$$b_n = \frac{2}{N} \sum_{k=1}^{N} X_k \sin\frac{2\pi nk}{N}$$

The quantity that is used to represent the spectrum is the power spectral density, Φ_n,

$$\Phi_n = \frac{T}{2}(a_n^2 + b_n^2)$$

where T is the length in units of time of the record being analyzed. If the phenomenom being investigated was sampled at an interval of Δ, then the Nyquist frequency (i.e., the highest frequency for which the spectrum can be resolved) is $1/(2\Delta)$. The lowest frequency for which the spectrum can be resolved is $1/T$ where T can also be represented as ΔN. To increase the confidence that can be placed in the power spectral density estimates and also to decrease the number of estimates (there are N/2 raw estimates), they are averaged in equal, logorithmically spaced frequency bands. Both 6 and 12 bands per decade of frequency are used in this study.

Confidence intervals at the 95% level for the band averaged spectral estimates, $\bar{\Phi}$, are calculated by assuming a chi-squared distribution for the estimates. An equivalent degrees of freedom, is calculated for each $\bar{\Phi}$,

$$\nu = \frac{2\bar{\Phi}^2}{\text{variance}[\bar{\Phi}]}$$

If $\tilde{\Phi}$ is the true value of the power spectral density, then the confidence limits are estimated as

$$\frac{\nu\Phi}{X_{\nu:0.025}} < \tilde{\Phi} < \frac{\nu\Phi}{X_{\nu:0.975}}$$

where the chi-squared values are approximated by using the following formulas

$$X_{\nu:0.025} \simeq \nu(1 + 9.892\nu^{-3.4})\,(1-2/(9\nu) - 1.96(2/(9\nu))^{1/2})^3$$

$$X_{\nu:0.975} \simeq \nu\,(1 - 2/(9\nu) + 1.96\,(2/(9\nu))^{1/2})^3$$

It is assumed in carrying out the spectral analysis that the time series are stationary (i.e., the moments do not change with time) and that they have been sampled at an interval, Δ, which is one-half the length of the shortest fluctuation present. In this work the time series were examined to insure that they were reasonably stationary. The sampling interval of 30 seconds was fixed. This resulted in the instantaneous wind speed not being adequately sampled which caused severe aliasing problems in the spectra calculated for this signal. The time averaged wind speed did not have this problem due to the 60 second time constant in the analog averaging circuit. The one-half hour mean time series were carefully edited to replace any bad data prior to analysis. The spectra for the 30 second per sample data was very easily contaminated by non-stationarities such as spikes or

trends. Baer and Withee (1971) and our own experience show that these problems, depending on their severity, can grossly distort the spectrum. The general characters of air temperature and wind spectra are known and any results must be physically meaningful, so that bad runs of spectral computations were eliminated by visual inspection.

Bath (1974) is an exceptionally good text covering the spectral analysis of geophysical data, and it was used extensively in developing the methods used here. Appendix A in the thesis of Andreas (1977) is a good summary of the philosophy and the mathematical derivation of applied spectral analysis. All spectral estimates in this study were computed using the Fast Fourier Transform (FFT) based on the Cooley and Tulkey (1965) algorithm.

There are two common representations in the literature for the graphing of mesoscale and synoptic-scale meteorological spectra. One can plot $\log \Phi$ vs. $\log f$, where f is the frequency, or $f\Phi$ vs $\log f$. The advantage of the first is that the power laws are represented by straight lines. The second has the advantage that equal areas under the curve contribute equally to the total variance of the time series. Both representations are used in the following sections. The statistics and other pertinent information for all of the spectra that follow, except for the composite wind speed spectrum and the wind component spectra, are contained in Table III.

TABLE III. Means and Variances of the Time Series Used in Calculating Spectra.

Figure	Variable	Length	Camp	Period	Mean	Variance
7	Wind Speed	16384	Bluefox	30 Apr 75 - 5 Apr 76	4.8 m s^{-1}	4.5 $m^2 s^{-2}$
8	Wind Speed	4096	Caribou	1 Jun 75 - 26 Aug 75	4.7 m s^{-1}	4.9 $m^2 s^{-2}$
8	Wind Speed	4096	Caribou	9 Aug 75 - 2 Nov 75	5.6 m s^{-1}	6.9 $m^2 s^{-2}$
8	Wind Speed	4096	Caribou	5 Nov 75 - 29 Jan 76	4.6 m s^{-1}	5.5 $m^2 s^{-2}$
8	Wind Speed	4096	Caribou	25 Jan 76 - 19 Apr 76	4.5 m s^{-1}	5.1 $m^2 s^{-2}$
9	Time Average Wind Speed	8192	Caribou	7 Jul 75 - 9 Jul 75	6.2 m s^{-1}	6.4 $m^2 s^{-2}$
9	Time Average Wind Speed	8192	Caribou	28 Dec 75 - 30 Dec 75	3.7 m s^{-1}	1.7 $m^2 s^{-2}$
9	Time Average Wind Speed	8192	Snowbird	28 Jan 76 - 30 Jan 76	6.8 m s^{-1}	7.0 $m^2 s^{-2}$
9	Time Average Wind Speed	8192	Bluefox	14 Mar 76 - 16 Mar 76	4.9 m s^{-1}	1.2 $m^2 s^{-2}$
15	Temperature 9m	16384	Bluefox	30 Apr 75 - 5 Apr 76	-18.2° C	199.6° C^2
16	Temperature 9m	4096	Bluefox	1 Jun 75 - 26 Aug 75	-10.4° C	3.9° C^2
16	Temperature 9m	4096	Bluefox	9 Aug 75 - 2 Nov 75	-9.6° C	75.3° C^2
16	Temperature 9m	4096	Bluefox	5 Nov 75 - 29 Jan 76	-31.9° C	32.6° C^2
16	Temperature 9m	4096	Bluefox	25 Jan 76 - 19 Apr 76	-30.0° C	46.1° C^2

3.2 Wind Speed Spectra

Figure 7 shows the spectrum calculated from a single 16,384-point (341 days) time series of one-half hour mean wind speed. This particular spectrum is from Bluefox, but the spectra from the other two camps are nearly identical. This figure is in basic agreement for periods of a day and longer with the wind speed spectrum calculated by Dorman (1974) from data collected at Ocean Weather Station N located at 30°N, 140°W. The $f \cdot \Phi$ vs log f representation of the spectrum in Figure 7 is contained in the composite spectrum of Figure 11. It is worthwhile to note the lack of a diurnal peak in Figure 11. Most investigators who have studied surface (normally near ten meters height) wind speed spectra over land have found a peak at a day (Petersen, 1975; Oort and Taylor, 1969; Lyons, 1975). The lack of a diurnal peak can be attributed to the lack of significant diurnal heating and cooling of the surface for both water and ice. Our spectrum shows a broad peak of magnitude 1.8 $m^2 s^{-2}$ for periods between 3 and 12 days. This compares to a level of 1 to 3 $m^2 s^{-2}$ for periods of 2 to 8 days for the various spectra of Oort and Taylor for continental U.S. weather stations. Van der Hoven (1957) found a value of 5 $m^2 s^{-2}$ at a height of 100 meters for the same time periods. Dorman found a peak of near 3 $m^2 s^{-2}$ centered at about 8 days.

Seasonal wind speed spectra are presented in Figure 8. These

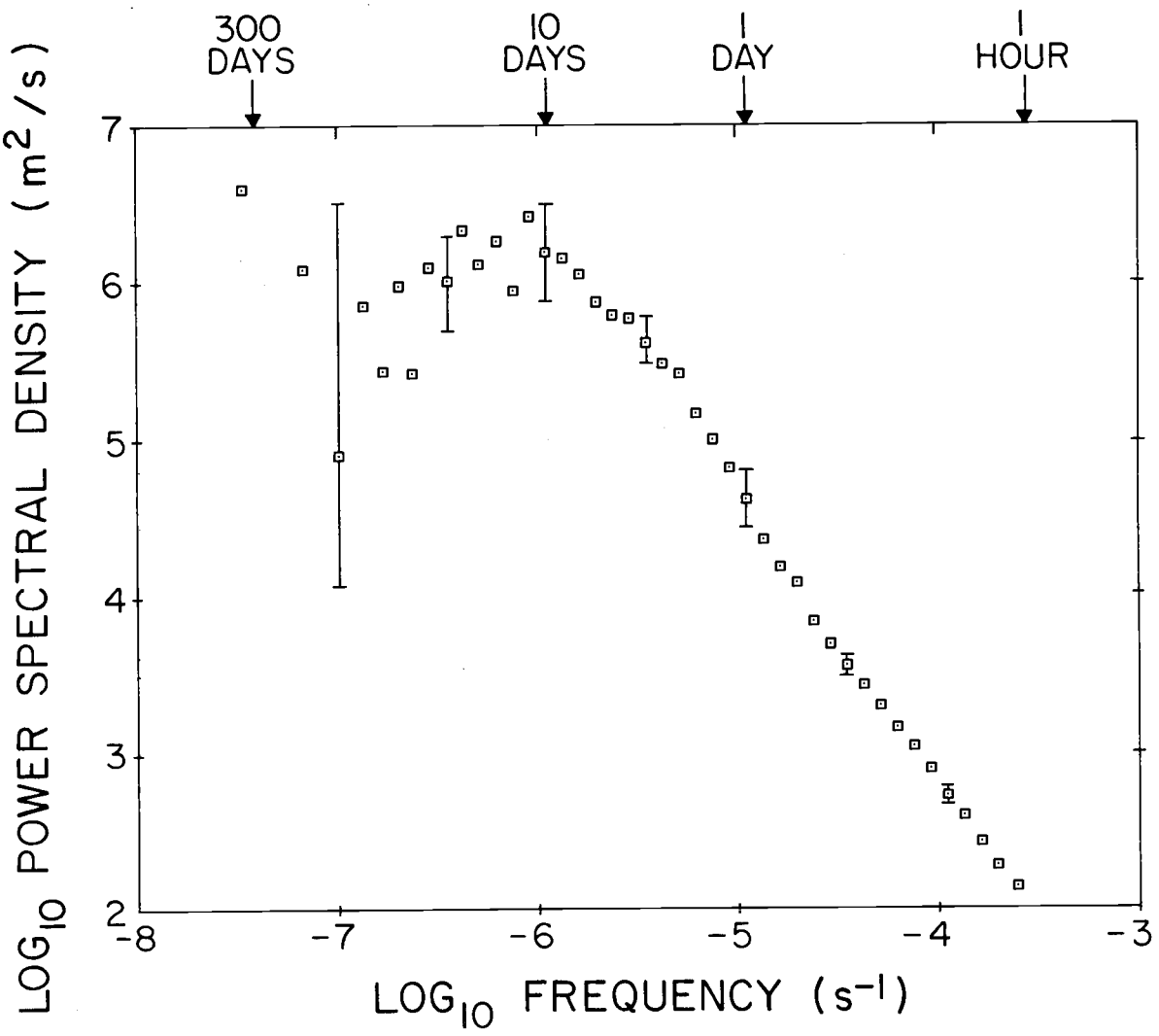

Figure 7. Wind speed spectrum from a 341-day series of one-half hourly means from Bluefox, log Φ vs log f. Confidence bars are at the 95% level.

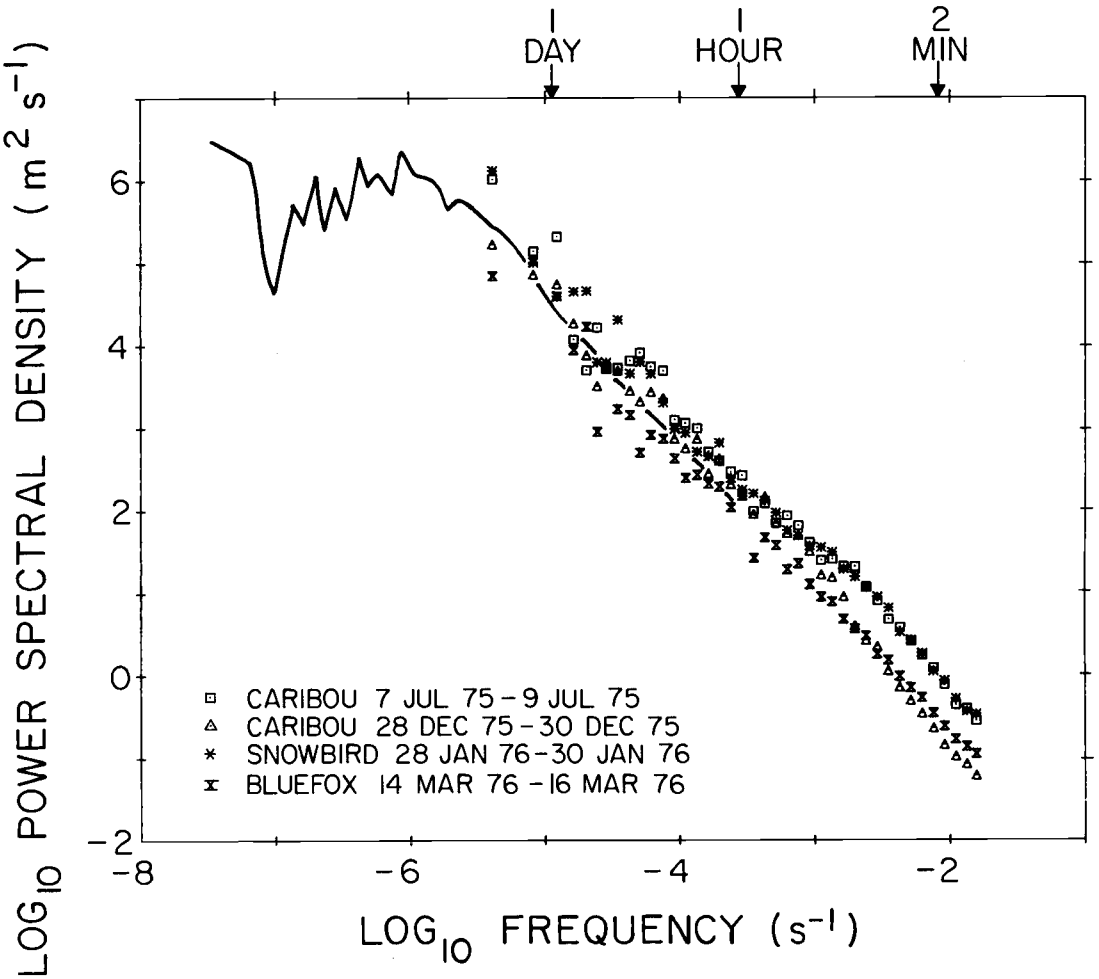

Figure 8. Wind speed spectra from four seasons, four 84-day series of one-half hourly means from Caribou, log Φ vs log f.

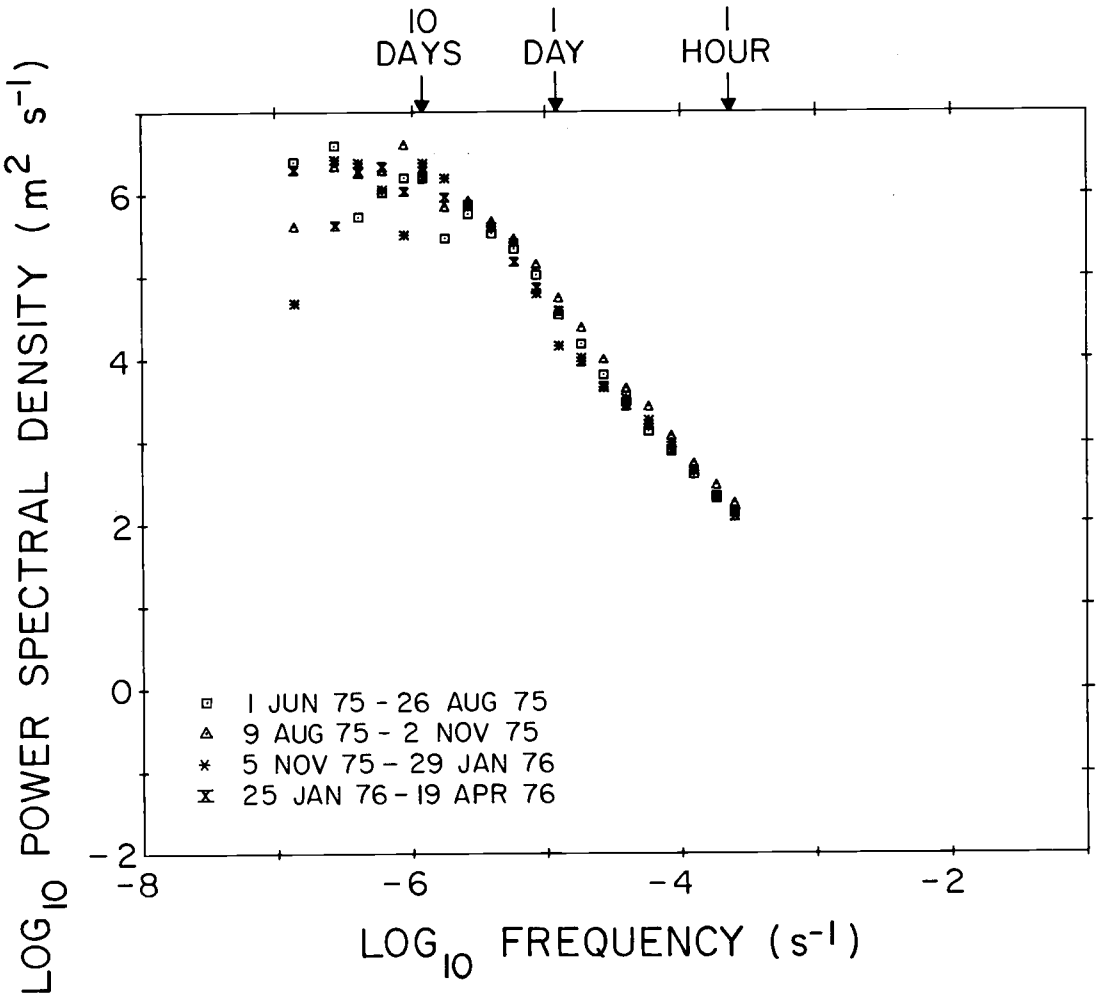

Figure 9. Wind speed spectra for four series, two samples per minute 2.8 days in length, log Φ vs log f. The solid line represents the spectrum of Figure 7.

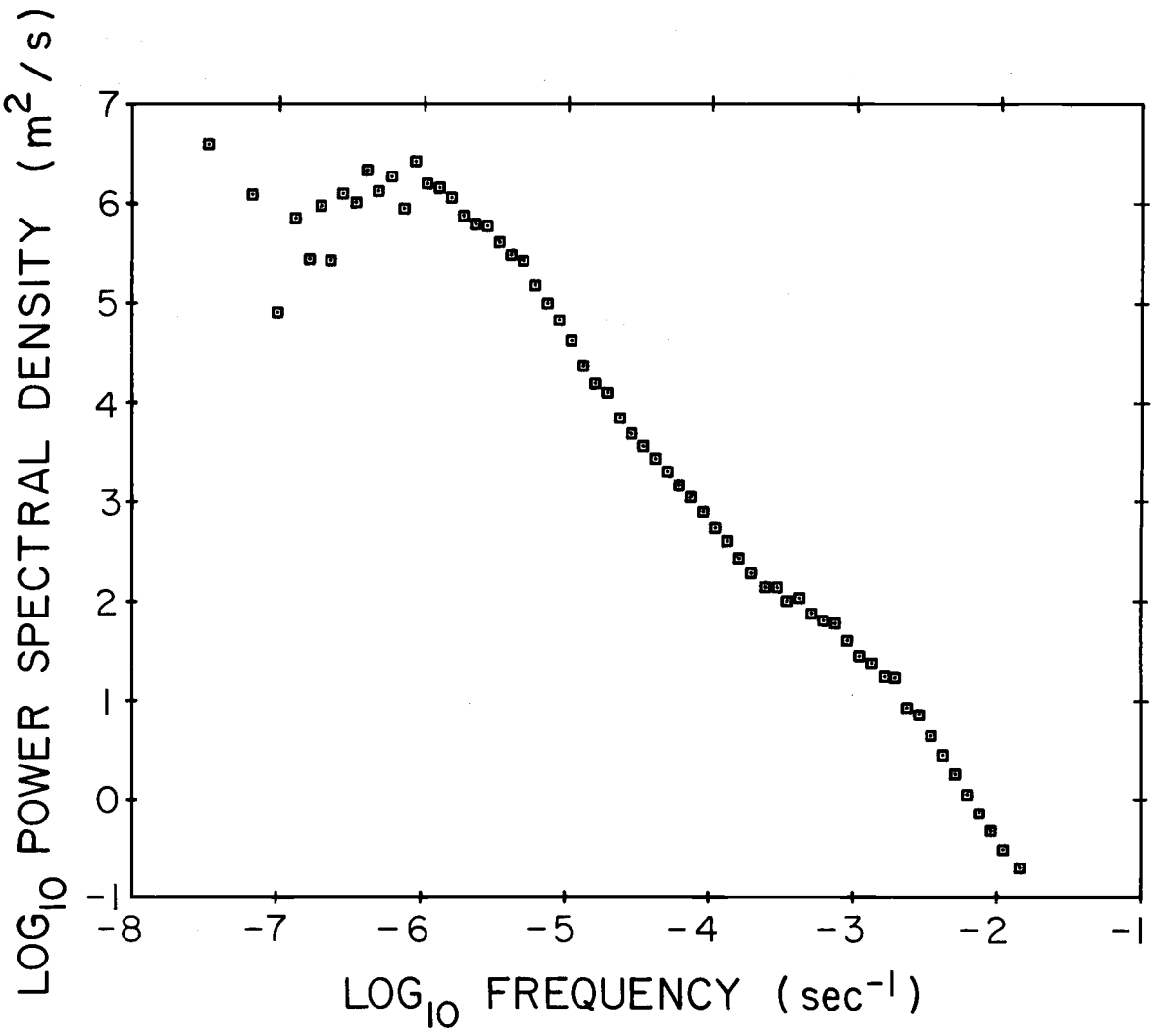

Figure 10. Composite wind speed spectrum for periods from one minute to 341 days, log Φ vs log f.

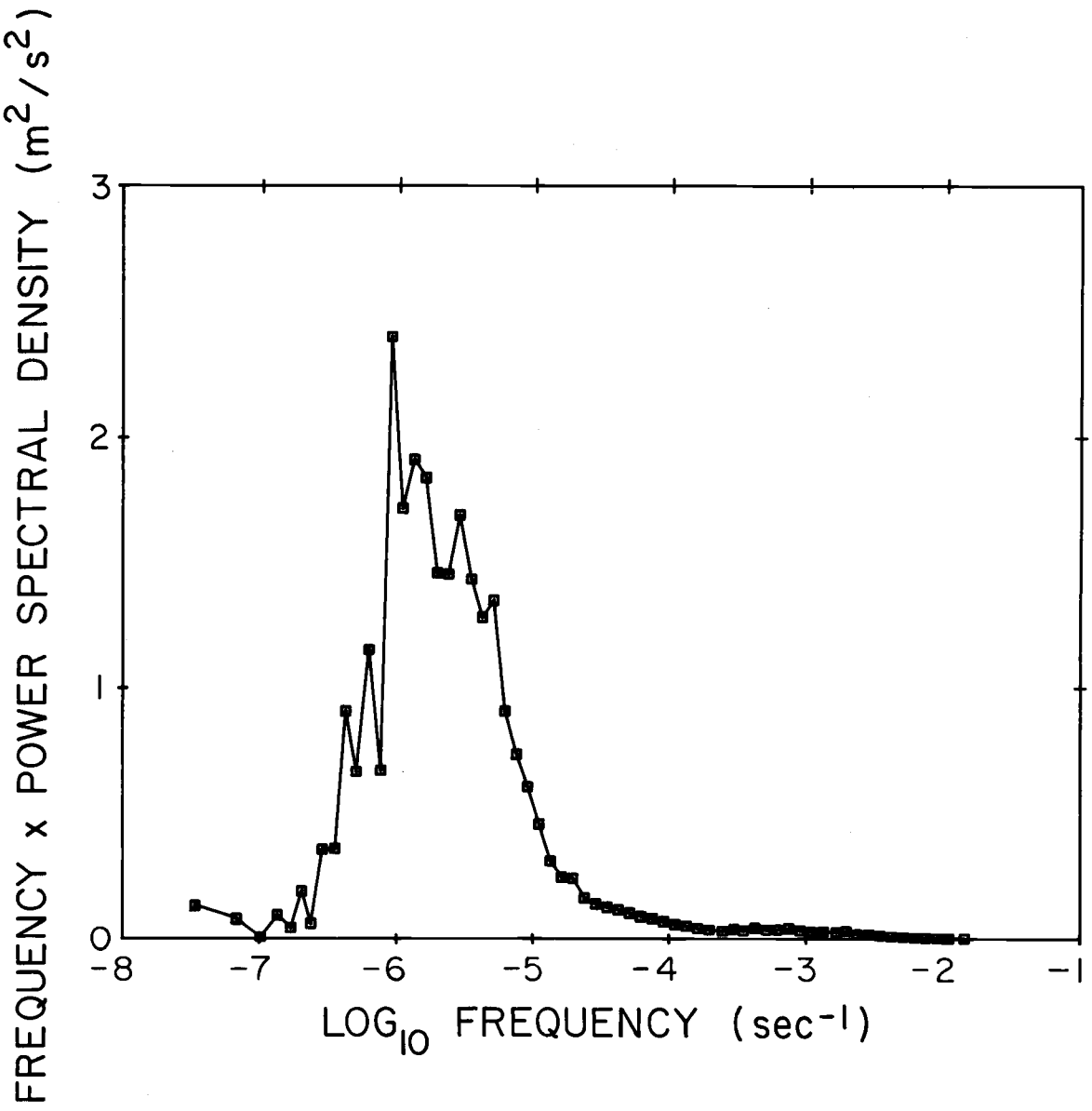

Figure 11. Composite wind speed spectrum for periods from one minute to 341 days, f· Φvs log f.

are 4096 point (84 days) series of one-half hour means. It is important to note that there is very little variation in spectral levels between seasons. In the $f \cdot \phi$ vs log f plot, which is not shown, there is a lack of a significant diurnal peak for all seasons. Dorman in his work found much more energy present in the winter spectra than the summer, with the spring and fall spectral values being transitional. Lyons (1957) found that on the south coast of Australia there was a strong peak (4.8 $m^2 s^{-2}$) at one day for the summer wind speed spectrum resulting from a local land-sea breeze system. For the winter spectrum he found a synoptic peak (3 days) of 2.9 $m^2 s^{-2}$. The AIDJEX data shows a peak of about 2 $m^2 s^{-2}$ centered at 5 days for all seasons.

In Figure 9 the spectra from four 8192 point (2.8 days) series of the time-averaged, 30-second wind speed data are presented. While significant variations in levels are present, these variations are related to the variation in the mean wind speed. At the high-frequencies, the spectra fall off more rapidly than $f^{-5/3}$, perhaps because of stable stratification.

In Figure 10 an attempt has been made to patch together a composite spectrum for time periods from 1 minute to 341 days. These spectral values are an average of the band-averaged power spectral densities from several runs of half hour mean and 30 second per sample spectra. Each band averaged value was weighted

according to the number of raw estimates in its band. The $f \cdot \Phi$ vs log f representation of this spectrum is contained in Figure 11.

Over land there is expected to appear in the $f \cdot \Phi$ vs log f representation of the wind speed spectrum a peak in the microscale centered about a period of one minute if there is sufficient shear or buoyantly driven turbulence (Fiedler and Panofsky, 1970). This is separated from the synoptic peak by the so-called "spectral gap" resulting from the lack of a mechanism for the generation of motion at the mesoscale. Figure 11 and many other spectra that were calculated from the AIDJEX data but have not been presented do not give any indication of a significant rise in spectral levels towards the high frequency end of the spectrum. However, our Nyquist frequency of $1/60\ s^{-1}$ does not allow us to make a definite statement. Considering the stably stratified surface layer atmosphere and the rather smooth surface found in the Arctic, it is not surprising that microscale turbulence is not consistently generated, even with the moderate wind speeds that are normally present. There are phenomena, however, such as open leads which expose relatively warm (-1.6°C) water to the very cold air that can locally create very unstable conditions (Andreas, 1977) and thereby generate microscale turbulence.

3.3 Wind Component Spectra

Up to this point only the spectra of the horizontal wind speed has

been considered. Petersen (1975) in a very thorough study has shown that an analysis of wind speed data alone does not truly represent the division of the total kinetic energy (i.e., total kinetic energy is the mean squared plus the variance) into eddy kinetic energy (variance) and mean flow kinetic energy. For a given wind record, both a vector (wind component) analysis and a wind speed analysis will contain the same total kinetic energy. However, if wind direction fluctuations are large, more of the energy will be in the summed variance of the component series then in the wind speed series. Based on the assumption that the fluctuating part of the velocity is small, compared to the mean,

$$u = \bar{u} + u'$$

$$u' << \bar{u}$$

the following expression can be derived,

$$\sigma_u^2 + \sigma_v^2 \simeq \sigma_{|u|}^2 + |u|\, \sigma_\beta^2$$

This states that the sum of the variances from the u and v component series is approximately equal to the variance of the wind speed only if the fluctuations in the wind direction, β, are very small. For synoptic time scales where the wind direction varies considerably, the integrated sum (variance) of the component spectral values is expected to be much larger than the integrated wind speed spectral values.

Figure 12 is a $f \cdot \Phi$ vs log f plot of the spectra of the u component (Φ_u), v component (Φ_v), wind speed ($\Phi_{|u|}$), and the summed spectra of the u and v component series ($\Phi_u + \Phi_v$) for Snowbird. There is an 80% loss of eddy kinetic energy in going from $\Phi_u + \Phi_v$ to $\Phi_{|u|}$ (i.e., the integrated spectrum for $\Phi_u + \Phi_v$ is 80% larger than the integrated spectrum for $\Phi_{|u|}$). The log Φ vs log f plot for $\Phi_u + \Phi_v$ and $\Phi_{|u|}$ is Figure 13. The shapes of the two are very similar although there is a consistent offset in levels. The statistics of the component spectra are contained in Table IV.

In the Arctic the major contribution to the variance of the wind record results from the wind direction fluctuations of the synoptic weather systems. This was found to also be the case in mid-latitudes by Petersen (1975). A diurnal peak is missing in the spectra of the wind components (as was the case for the wind speed spectra) reconfirming the lack of a significant daily fluctuation in the wind field for the AIDJEX data.

3.4 Air Temperature Spectra

Spectra of air temperature were calculated for the interval of 1 hour to 341 days. The 0.08°C resolution of the data acquisition system was too large to allow confidence in the spectra calculated from the data sampled twice per minute, therefore none are presented. The log Φ vs log f representation of the one-half hour mean

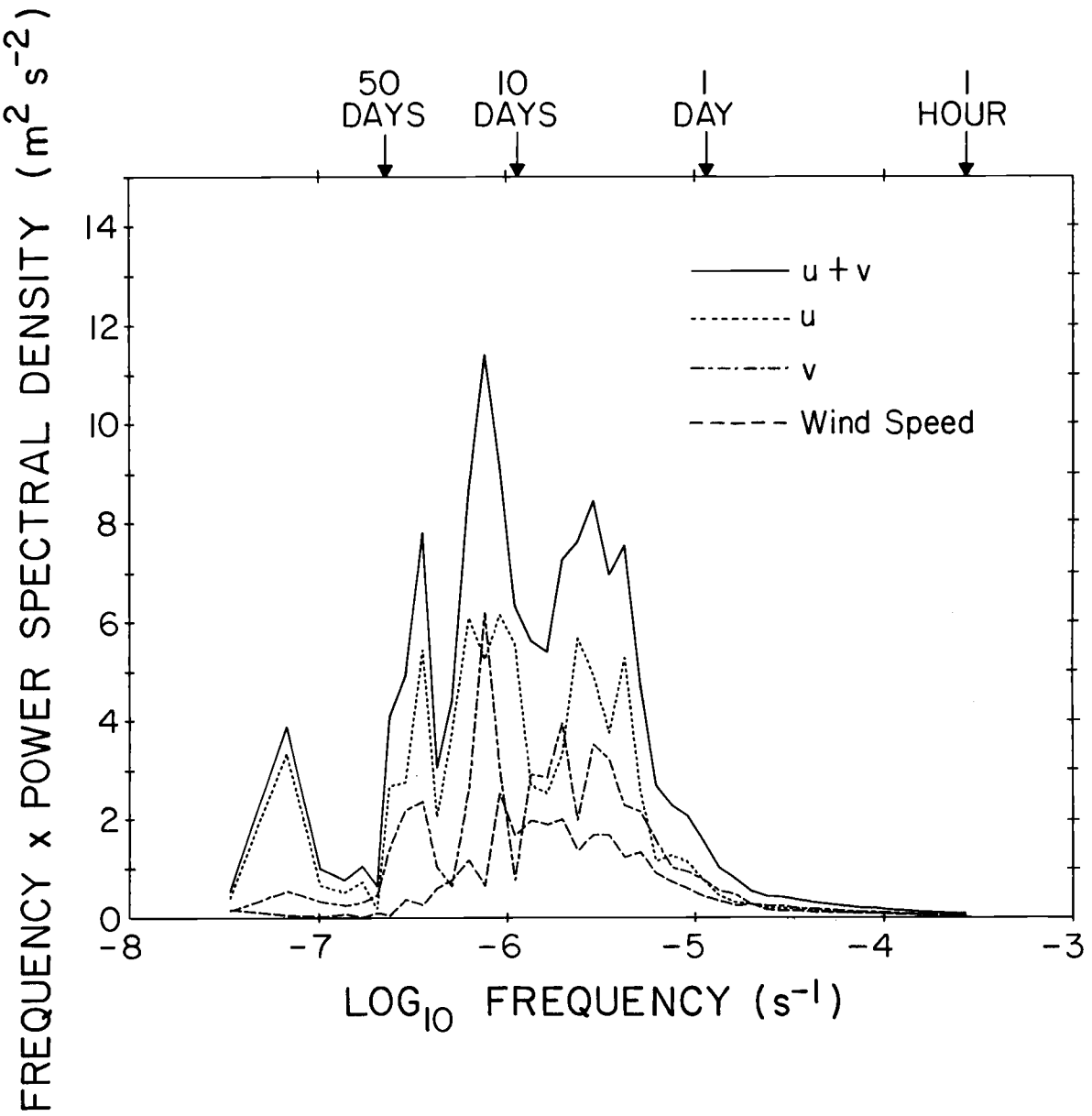

Figure 12. Wind component, wind speed, and summed wind component spectra from a 341-day series of one-half hourly means from Snowbird, $f \cdot \Phi$ vs log f.

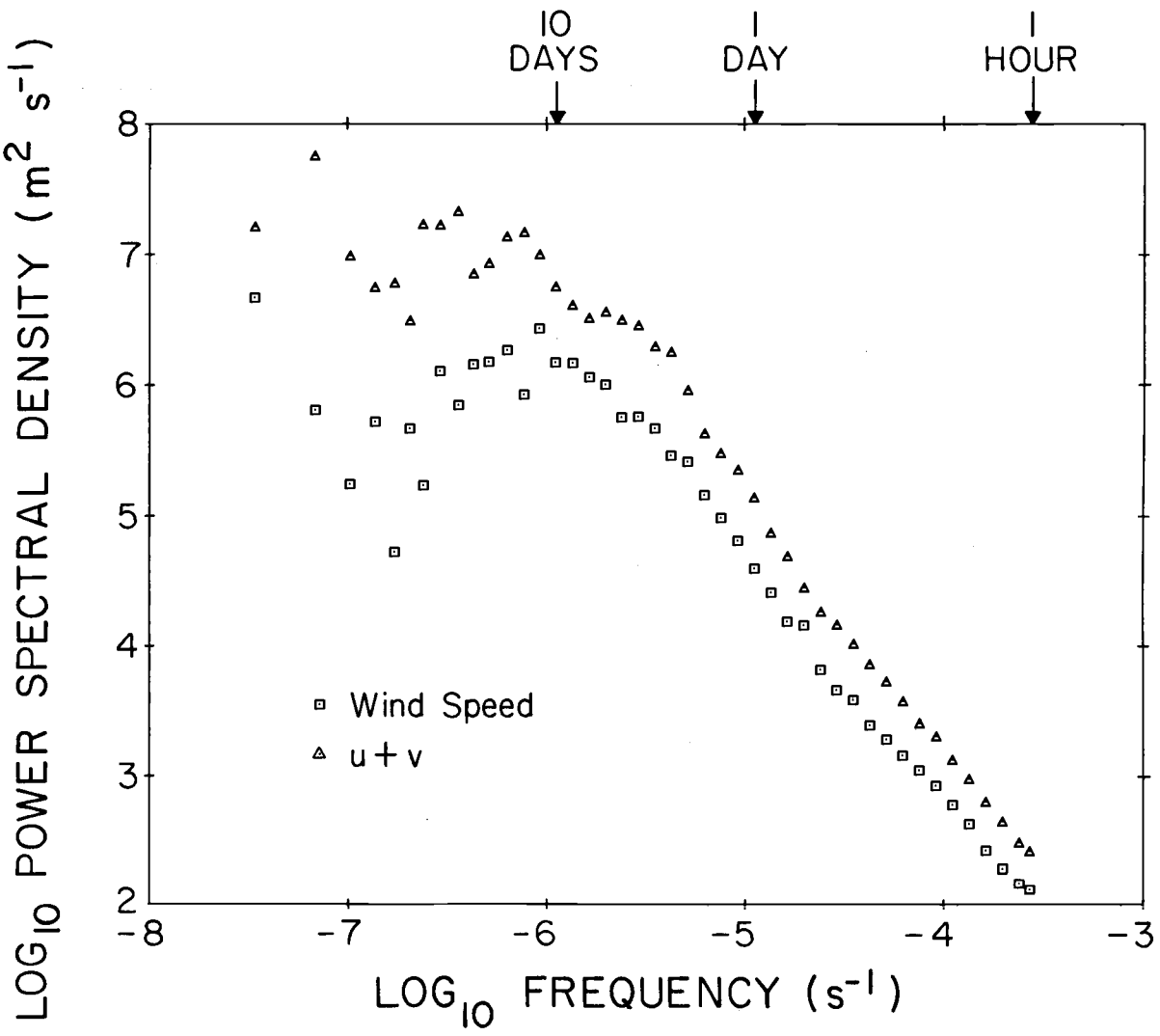

Figure 13. Wind speed and summed wind component spectra from 341-day series of one-half hourly means from Snowbird, log Φ vs log f.

TABLE IV. Wind Component and Wind Speed Statistics.
All values are from 16834 point series of one-half hour means covering the period 30 April 1975 to 5 April 1976. Units are m s^{-1} for the means and $m^2 s^{-2}$ for the means squared and variances.

	Caribou			Bluefox			Snowbird		
	Mean	Mean Squared	Variance	Mean	Mean Squared	Variance	Mean	Mean Squared	Variance
u	0.280	0.078	19.662	0.572	0.327	17.307	0.295	0.087	17.306
v	-0.445	0.198	9.262	-0.432	0.187	9.786	-0.482	0.232	10.278
wind speed	4.880	23.814	5.641	4.833	23.844	4.516	4.802	23.059	5.141
u + v	-0.164	0.027	30.584	0.140	0.020	27.511	-0.188	0.035	28.086

air temperature spectrum is given in Figure 14. This spectrum was calculated from a single 16,384 point (341 days) series from the nine meter temperature sensor at Bluefox. The seasonal spectra for Bluefox are presented in Figure 15. We find that the summer values are an order of magnitude less than those in the other three seasons. This contrasts with the findings of Dorman (1974) who found spring and fall to be transitional between the highest values found in winter and the lowest values found in summer. The summertime surface conditions in the Arctic account for the very low variance found in the temperature signal for this season. The spectral levels in this study (i.e., the value of Φ) are larger than Dorman's by one or two orders of magnitude, but compare with the observations over land of Petersen (1975) and Kolesnikova and Monin (1965).

Between periods of 1 day and 1 hour, the spectra fall off proportional to $f^{-2.7}$, in disagreement with the wind spectra which falls off in the same period proportional to $f^{-5/3}$ (Figure 7).

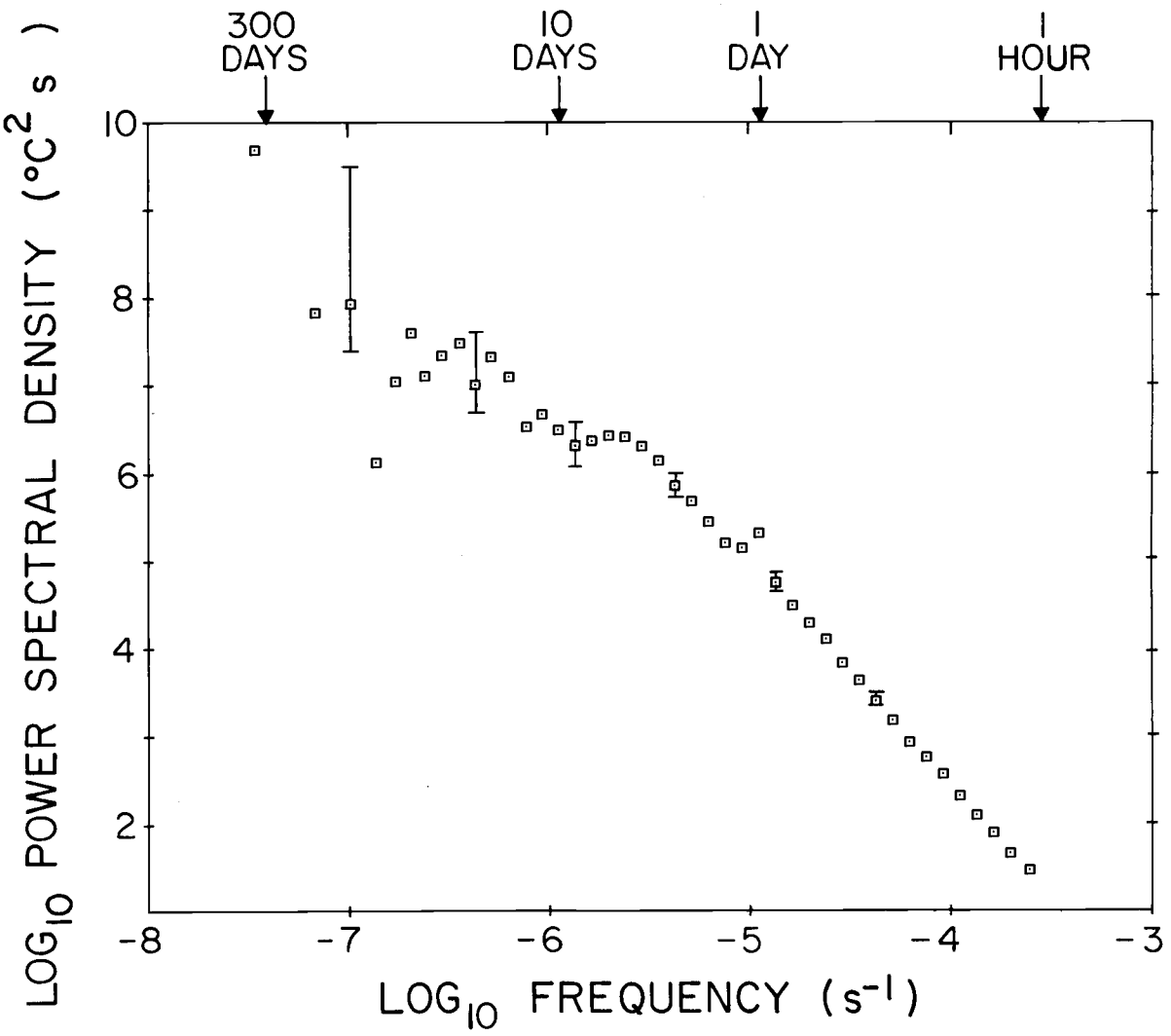

Figure 14. Air temperature spectrum from a 341-day series of one-half hourly means from Bluefox, log Φvs log f. Confidence bars are at the 95% level.

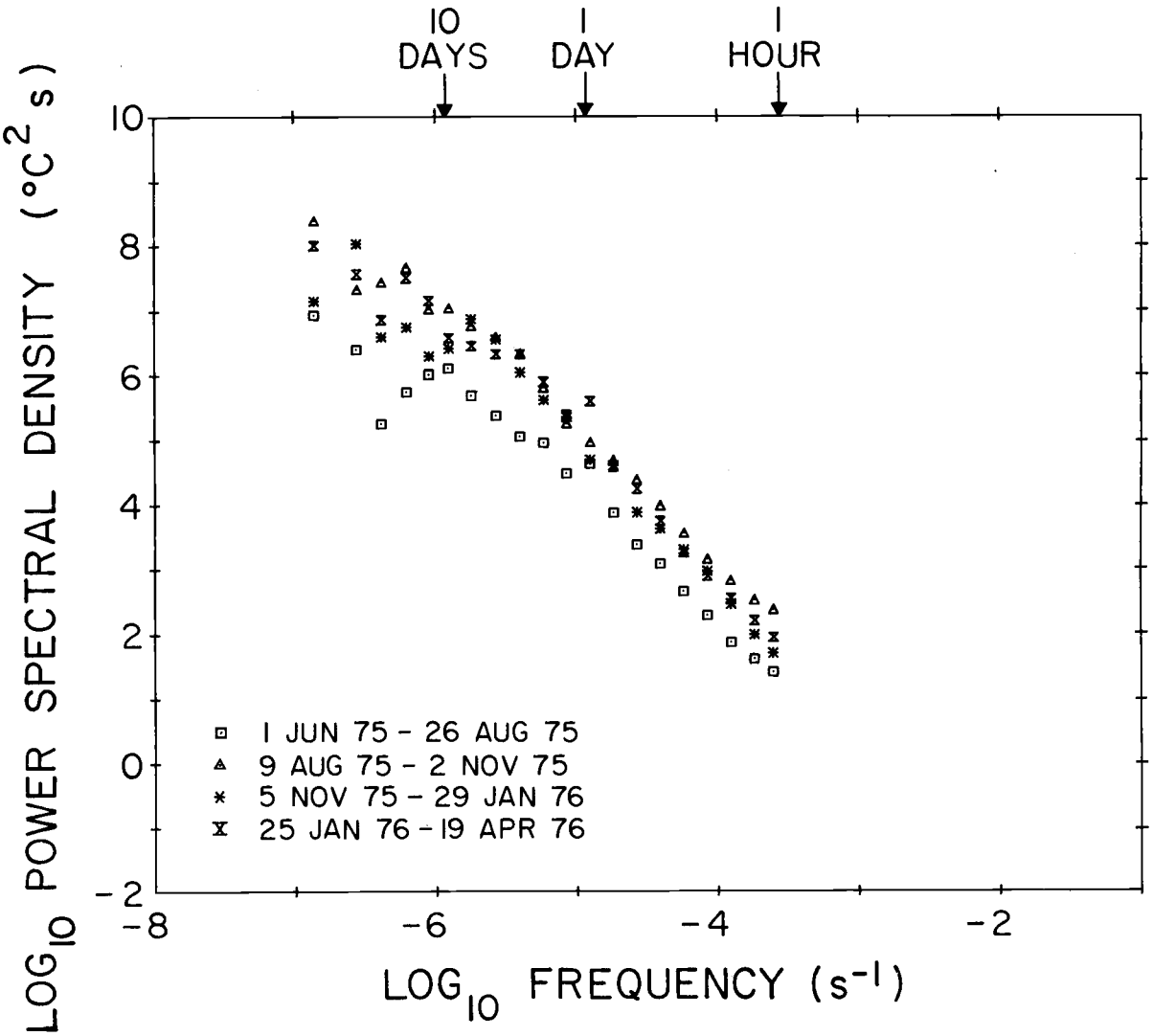

Figure 15. Seasonal air temperature spectra for 84-day series of one-half hourly means from Bluefox, log Φ vs log f.

4. DIVERGENCE AND VORTICITY

4.1 Introduction

The data collected during the AIDJEX main experiment provide a unique opportunity to investigate long term series of the horizontal divergence and the vertical component of vorticity for both the wind field and ice motion. The positions of the camps were measured with an accuracy of ± 20 m (Thorndike and Cheung, 1977) by a satellite navigation system. The ice velocity time series was derived from the positioning information and was provided along with the position time series by the AIDJEX office at the University of Washington. A thorough discussion of these series is given by Thorndike and Cheung (1977). The wind vector used was the daily mean series calculated from the instantaneous wind speed and direction sampled twice per minute. Because of the high latitudes (72° - 76° N) in which the experiment took place, the convergence of the meridians in a latitude, longitude coordinate system could not be ignored (Panofsky, 1946). Therefore, all variables were transformed into a cartesian coordinate system based on the Greenwich meridian as the positive X axis and 90° E longitude as the positive Y axis (see Appendix 7, Thorndike and Cheung, 1977).

Using a two-dimensional Gauss' theorem and some vector algebra, an average horizontal divergence can be defined as

$$\overline{(\nabla \cdot \underset{\sim}{u})} = \frac{1}{A} \oint u\, dy - v\, dx$$

where u and v are the average velocity components from two camps defining a side of the triangular array, A is the area of the triangle, and the integration path is counterclockwise. If the three camps are identified by 1, 2, and 3, the actual computation is,

$$\overline{(\nabla \cdot \underset{\sim}{u})} = \frac{1}{2A} [(u_1 + u_2)(y_2 - y_1) - (v_1 + v_2)(x_2 - x_1) + (u_2 + u_3)$$
$$(y_3 - y_2) - (v_2 + v_3)(x_3 - x_2) + (u_3 + u_1)(y_1 - y_3) -$$
$$(v_1 + v_3)(x_1 - x_3)].$$

Likewise by Stoke's theorem, an average vertical component of vorticity is defined as,

$$\overline{(\nabla x \underset{\sim}{u})}_k = \frac{1}{A} \oint u\, dx + v\, dy$$

which translates into the computational equation

$$\overline{(\nabla x \underset{\sim}{u})}_k = \frac{1}{2A} [(u_1 + u_2)(x_2 - x_1) + (v_1 + v_2)(y_2 - y_1) +$$
$$(u_2 + u_3)(x_3 - x_2) + (v_2 + v_3)(y_3 - y_2) + (u_3 + u_1)(x_1 - x_3)$$
$$(v_3 + v_1)(y_1 - y_3)].$$

The area of a triangle given the cartesian coordinates of the corners is

$$A = (x_1 y_2 + x_2 y_3 + x_3 y_1 - y_1 x_2 - y_2 x_3 - y_3 x_1).$$

A good discussion of the theory of the calculation of divergence and vorticity can be found in Bryden and Fofonoff (1977). It should be noted that the correction usually needed in divergence and vorticity calculations to compensate for the differing elevations of the measuring stations (Schaefer, 1973) are not needed in this study. The vorticity is positive for cyclonic (counterclockwise) flow and negative for anticyclonic (clockwise) flow.

4.2 Discussion

The time series for the daily averaged divergence and vorticity of the wind field for a period of 356 days are presented in Figure 16. The correlation coefficient between the two series, -0.65, indicates strong negative correlation. For the AIDJEX data there is an almost complete lack of a significant daily cycle in the wind field and this is reflected in the divergence and vorticity series. From Figure 16 the values of divergence and voriticty are seen to fluctuate on the synoptic time scale. Burt et al. (1977) found that for wind data recorded over the ocean the divergence and vorticity vary roughly as L^{-1} where L is the length scale over which the calculations were made. If the average length scale of the AIDJEX manned camp array is chosen to be 200 km, then L^{-1} is $5 \times 10^{-6} m^{-1}$. From Table V the mean absolute value of the divergence and vorticity are seen to be in rough agreement with this value.

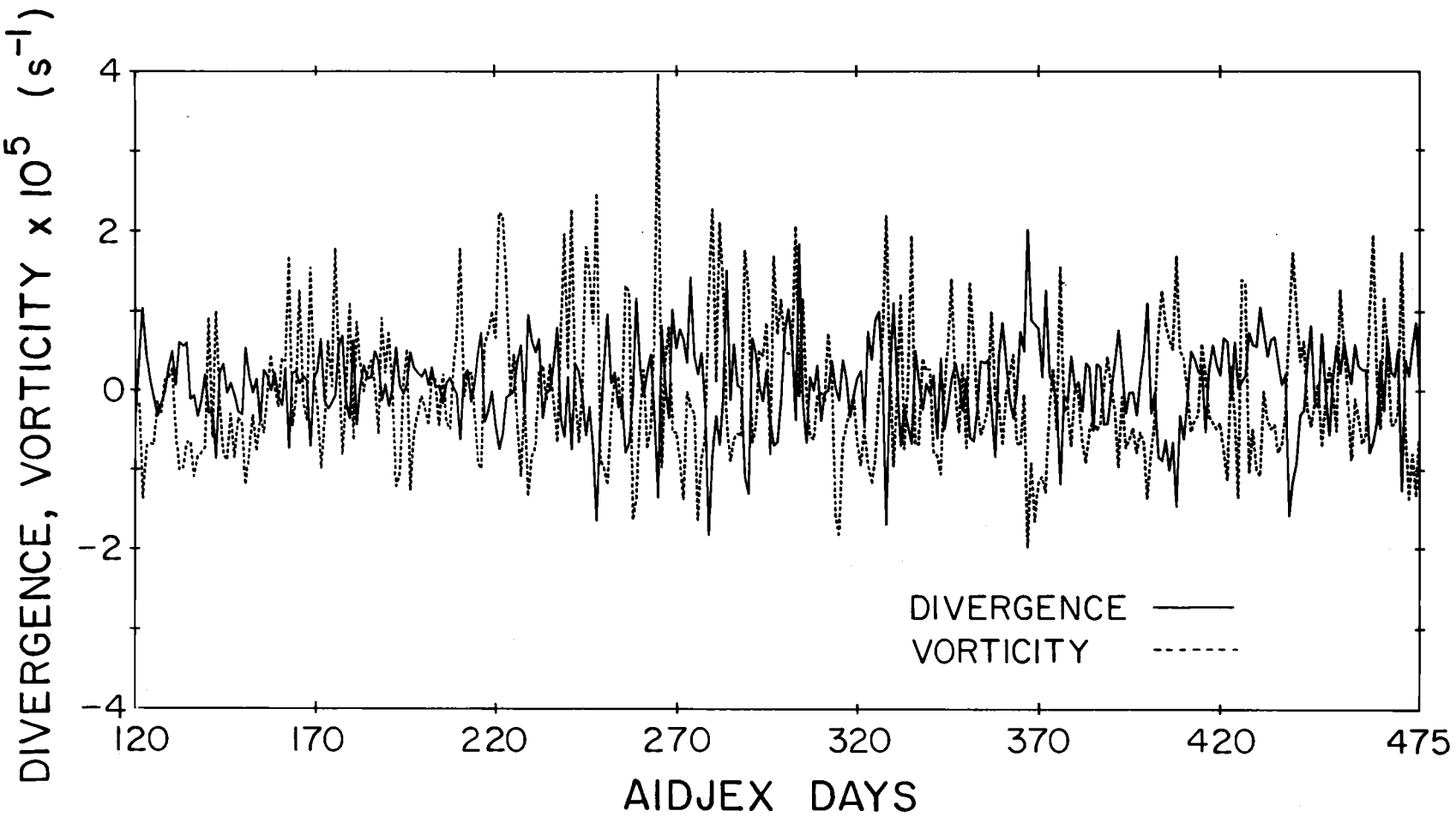

Figure 16. Time series of daily averaged divergence and vorticity of the wind field.

TABLE V. Statistics of the Daily Averaged Divergence and Vorticity Time Series. (Units are s^{-1})

	Mean	Mean of the absolute values	Variance	Variance of the absolute values
Wind Divergence	6.3×10^{-7}	4.1×10^{-6}	5.3×10^{-6}	3.5×10^{-6}
Wind Vorticity	-5.2×10^{-7}	6.7×10^{-6}	8.6×10^{-6}	5.4×10^{-6}
Ice Divergence	1.1×10^{-9}	5.2×10^{-8}	8.5×10^{-8}	6.7×10^{-8}
Ice Vorticity	-4.6×10^{-8}	1.2×10^{-7}	1.7×10^{-7}	1.3×10^{-7}

Correlation Coefficients

Wind divergence - wind vorticity	-0.65
Ice divergence - ice vorticity	0.22
Ice vorticity - wind vorticity	0.65
Ice divergence - wind divergence	0.00

The daily averaged divergence and vorticity time series for the ice motion are presented in Figure 17. The correlation coefficient between these two series is 0.22 which is not significant at the 95% level. This is not surprising when it is remembered that the ice is confined to moving on the horizontal plane while the air can move in the vertical as well. There are short periods, however, especially near the end of the experiment where the ice motion divergence and vorticity are well correlated negatively. The ice and wind vorticity series are positively correlated (0.65) while the ice and wind divergence series are not significantly correlated. Again, this is related to the fact that the ice can only move in a plane. The ice rotates but it resists piling up under the influence of the wind. Both the wind and ice vorticity series have a negative average value reflecting the well-documented anticyclonic ice rotation in the Beaufort Sea.

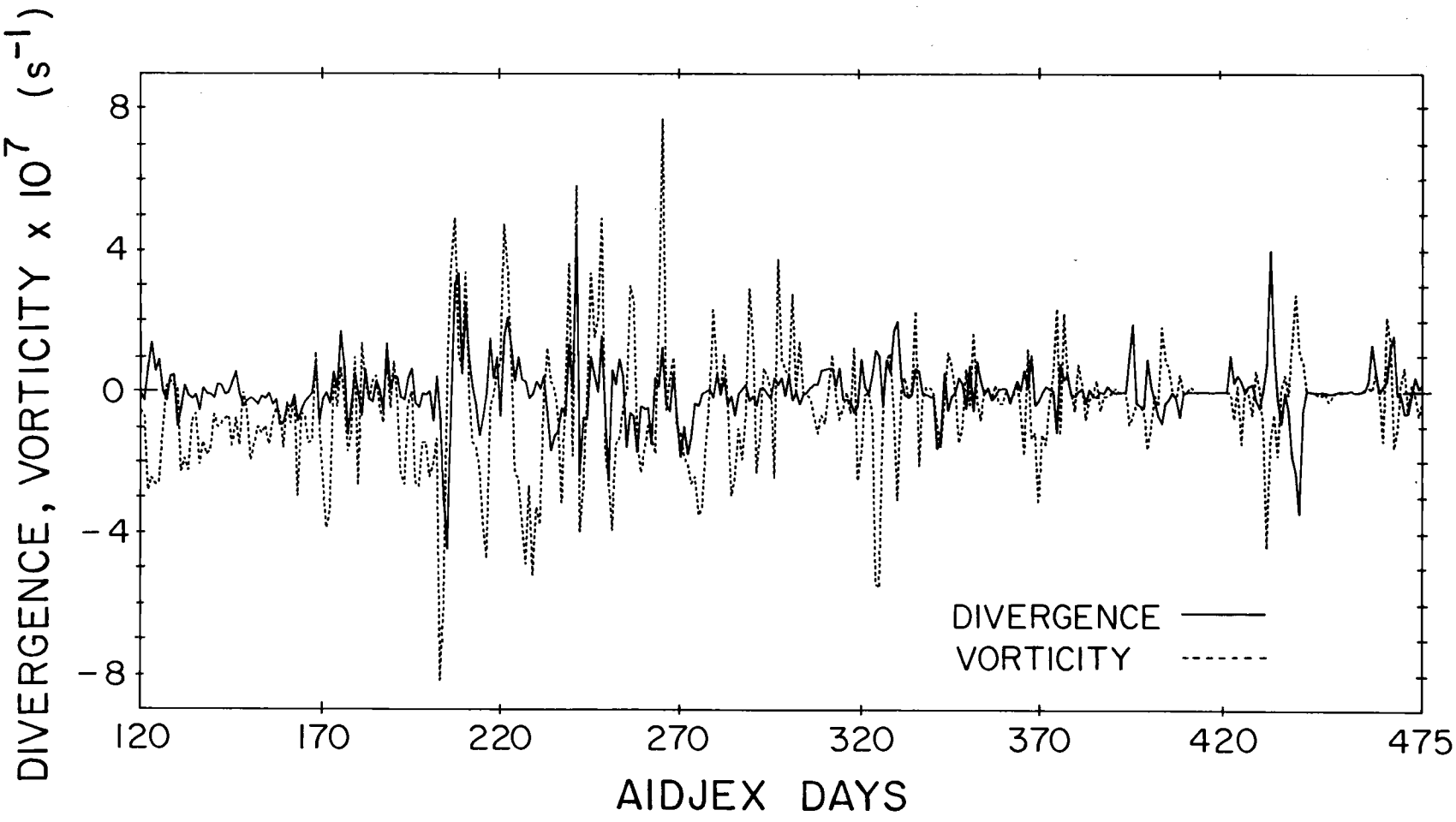

Figure 17. Time series of daily averaged divergence and vorticity of the ice motion.

5. SUMMARY

From data collected on the pack ice of the Beaufort Sea during the AIDJEX main experiment, year-long time series of air temperature and wind speed have been constructed. The following conclusions can be drawn from the analysis of these time series:

1) There is no evidence of a diurnal variation in the wind field for any season,
2) there is a small diurnal variation in the air temperature for the late summer, early fall and spring seasons only,
3) there is very little seasonal variability in the wind,
4) comparison of the wind speed with the wind component spectra indicates that synoptic variations in wind direction contribute much more to the total variance of the wind record than do speed fluctuations,
5) a significant correlation (0.65) exists between ice and atmospheric vorticity,
6) a significant negative correlation (-0.65) exists between atmospheric vorticity and divergence,
7) no significant correlation exists between ice and atmospheric divergence.

BIBLIOGRAPHY

Andreas, E. L. 1977. Observations of velocity and temperature and estimates of momentum and heat fluxes in the internal boundary layer over Arctic leads. Ph. D. Thesis, Oregon State University. 263 p.

Baer, L. and G. W. Withee. 1971. A methodology for defining an operational synoptic temporal oceanic sampling system. II. Nonstationary conditions. J. App. Met. 10: 1061-1065.

Bath, M. 1974. Spectral analysis in geophysics. Amsterdam. Elsevier. 563 pp.

Baumann, R. J. 1978. Documentation on the creation of the one-half hour mean meterological data tape for the AIDJEX main experiment, April 1975 to April 1976. Unpublished manuscript. Oregon State University.

Bryden, H. L. and N. P. Fofonoff. 1977. Horizontal divergence and vorticity estimates from velocity and temperature measurements in the MODE Region. J. Phys. Oceanogr. 7: 309-328.

Burt, W. V., T. Cummings and C. A. Paulson. 1974. The Mesoscale wind field over the ocean. J. Geophys. Res. 79: 5625-5632.

Burt, W. V., T. Cummings and C. A. Paulson. 1977. The magnitude of the horizontal divergence and the vertical component of vorticity in the surface wind field over the ocean. Meteor. Mag. 106: 197-204.

Chen, W. Y. 1977. Analysis of vorticity and divergence fields and other meteorological parameters over Lake Ontario during IFYGL. Mon. Wea. Rev. 105: 1298-1309.

Clarke, M., D. Bell, and E. Leavitt. 1977. Field calibration report, AIDJEX Meteorological Program April 1975 - April 1976. AIDJEX Bull. 36: 129-155.

Cooley, J. W. and J. W. Tukey. 1965. An algorithmn for the machine calculation of complex fourier series. Mathematics of Computation 19: 267-301.

Cummings, T. K. 1974. The mesoscale wind field during Project JASIN 1972. Masters Thesis. Oregon State University. 56 pp.

Dorman, C. E. 1974. Analysis of meteorological and oceanographic data from ocean station vessel N (30° N 140° W). Ph. D. Thesis. Oregon State University. 136 pp.

Fiedler, F. and H. A. Panofsky. 1970. Atmospheric scales and spectral gaps. Bull. Amer. Meteor. Soc. 51: 1114-1119.

Hwang, H. J. 1970. Power density spectrum of surface wind speed on Palmyra Island. Mon. Wea. Rev. 98: 70-74.

Kolesnikova, V. N. and A. S. Monin. 1965. Spectra of meteorological field fluctuations. Izv. Acad. Sci. USSR, Atmospheric and Ocean Physiscs Ser. (English Translation) 1: 653-669.

Lyons, T. J. 1975. Mesoscale wind spectra. Quart. J. R. Met. Soc. 101: 901-910.

Maykut, G. A., A. S. Thorndike, and N. Untersteiner. 1972. AIDJEX Scientific plan. AIDJEX Bull. 15: 1-67.

Millard, R. C., Jr. 1971. Wind measurements from buoys: a sampling scheme. J. Geophys. Res. 76: 5819-5828.

Oort, A. H. and A. Taylor. 1969. On the kinetic energy spectrum near the ground. Mon. Wea. Rev. 97: 623-636.

Panofsky, H. A. 1946. Methods of computing vertical motion in the atmosphere. J. Meteor. 3: 45-49.

Paulson, C. A. and D. Bell. 1975. Meteorological observations during the AIDJEX main experiment. AIDJEX Bull. 28: 1-10.

Petersen, E. L. 1975. On the kinetic energy spectrum of atmospheric motions in the planetary boundary layer. Danish Atomic Energy Commission Research Establishment RISØ, Report No. 285. 103 pp.

Schaefer, J. T. 1973. On the computation of the surface divergence field. J. App. Meteor. 12: 546-547.

Thorndike, A. S. and J. Y. Cheung. 1977. AIDJEX measurements of sea ice motion, 11 April 1975 to 14 May 1976. AIDJEX Bull. 35: 1-149.

Van der Hoven, I. 1957. Power spectrum of horizontal wind speed in the frequency range from 0.0007 to 900 cycles per hour. J. Meteor. 14: 160-164.

Vowinckel, E. and S. Orvig. 1970. The climate of the North Pole Basin. In: World Survey of Climatology, Vol. 14. S. Orvig, Editor, Amsterdam Elsevier. pp. 129-225.

APPENDIX

APPENDIX A

Conversion of Calendar Days to AIDJEX Days

Day of Month	Apr 1975	May 1975	Jun 1975	Jul 1975	Aug 1975	Sep 1975
1	91	121	152	182	213	244
2	92	122	153	183	214	245
3	93	123	154	184	215	246
4	94	124	155	185	216	247
5	95	125	156	186	217	248
6	96	126	157	187	218	249
7	97	127	158	188	219	250
8	98	128	159	189	220	251
9	99	129	160	190	221	252
10	100	130	161	191	222	253
11	101	131	162	192	223	254
12	102	132	163	193	224	255
13	103	133	164	194	225	256
14	104	134	165	195	226	257
15	105	135	166	196	227	258
16	106	136	167	197	228	259
17	107	137	168	198	229	260
18	108	138	169	199	230	261
19	109	139	170	200	231	262
20	110	140	171	201	232	263
21	111	141	172	202	233	264
22	112	142	173	203	234	265
23	113	143	174	204	235	266
24	114	144	175	205	236	267
25	115	145	176	206	237	268
26	116	146	177	207	238	269
27	117	147	178	208	239	270
28	118	148	179	209	240	271
29	119	149	180	210	241	272
30	120	150	181	211	242	273
31		151		212	243	

Appendix A. continued.

Day of Month	Oct 1975	Nov 1975	Dec 1975	Jan 1976	Feb 1976	Mar 1976	Apr 1976
1	274	305	335	366	397	426	457
2	275	306	336	367	398	427	458
3	276	307	337	368	399	428	459
4	277	308	338	369	400	429	460
5	278	309	339	370	401	430	461
6	279	310	340	371	402	431	462
7	280	311	341	372	403	432	463
8	281	312	342	373	404	433	464
9	282	313	343	374	405	434	465
10	283	314	344	375	406	435	466
11	284	315	345	376	407	436	467
12	285	316	346	377	408	437	468
13	286	317	347	378	409	438	469
14	287	318	348	379	410	439	470
15	288	319	349	380	411	440	471
16	289	320	350	381	412	441	472
17	290	321	351	382	413	442	473
18	291	322	352	383	414	443	474
19	292	323	353	384	415	444	475
20	293	324	354	385	416	445	476
21	294	325	355	386	417	446	477
22	295	326	356	387	418	447	478
23	296	327	357	388	419	448	479
24	297	328	358	389	420	449	480
25	298	329	359	390	421	450	481
26	299	330	360	391	422	451	482
27	300	331	361	392	423	452	483
28	301	332	362	393	424	453	484
29	302	333	363	394	425	454	485
30	303	334	364	395		455	486
31	304		365	396		456	